MOL #84558

Title Page

State-Dependent Etomidate Occupancy of its Allosteric Agonist Sites Measured in a Cysteine-Substituted GABA_A Receptor

Authors: Deirdre S. Stewart, Mayo Hotta, Rooma Desai, and Stuart A. Forman

Laboratory: Beecher-Mallinckrodt Research Labs, Department of Anesthesia Critical Care & Pain Medicine, Massachusetts General Hospital, Boston, MA, USA

Affiliations: Department of Anesthesia Critical Care & Pain Medicine, Massachusetts General Hospital, Boston, MA, USA (M.H., R.D, and S.A.F). Department of Anaesthesia, Harvard Medical School, Boston, MA, USA (S.A.F). Department of Neurobiology, Harvard Medical School, Boston, MA, USA (D.S.S.)

1

MOL #84558

Running Title Page

Running title: State-Dependent Protection of GABA$_A$R β2M286C by Etomidate

Corresponding author: Stuart A. Forman, Department of Anesthesia Critical Care & Pain

Medicine, Jackson 444, Massachusetts General Hospital, 55 Fruit Street, Boston, MA 02114.

Phone: 617-724-5156; Fax: 617-724-8644; E-mail: saforman@partners.org.

Text pages: 34

Tables: 1

Figures: 4

References: 25

Word counts:

Abstract: 246

Introduction: 640

Discussion: 1502

Non-standard abbreviations: GABA$_A$: γ-aminobutyric acid type A. SCAM: substituted

cysteine accessibility method. PCMBS: para-chloromercuribenzene sulfonate. PC$_{50}$: 50%

protective ligand concentration.

Abstract

A central axiom of ligand-receptor theory is that agonists bind more tightly to active than to inactive receptors. However, measuring agonist affinity in inactive receptors is confounded by concomitant activation. We identified a cysteine substituted mutant $GABA_A$ receptor with unique characteristics allowing determination of allosteric agonist site occupancy in both inactive and active receptors. Etomidate, the allosteric agonist, is an anesthetic that activates/modulates $\alpha1\beta2\gamma2L$ $GABA_A$ receptors *via* transmembrane sites near $\beta2M286$ residues in M3 domains. Voltage-clamp electrophysiology studies of $\alpha1\beta2M286C\gamma2L$ receptors show that GABA is an efficacious agonist, and etomidate modulates GABA-activated activity, but direct etomidate agonism is absent. Quantitative analysis of mutant activity using an established Monod-Wyman-Changeux (MWC) allosteric model indicates that the intrinsic efficacy of etomidate, defined as its relative affinity for active *vs*. inactive receptors, is lower than in wild-type receptors. Para-chloromercuribenzene sulfonate (pCMBS) covalently modifies $\beta2M286C$ sidechain sulfhydryls, irreversibly altering GABA-induced currents. Etomidate concentration-dependently reduces the apparent rate of $\beta2M286C$-pCMBS bond formation, tracked electrophysiologically. High etomidate concentrations completely protect the $\beta2M286C$ suflhydryl from covalent modification, suggesting close steric interactions. The 50% protective etomidate concentration (PC_{50}) is 14 μM in inactive receptors and 1.1 to 2.2 μM during GABA-activation, experimentally demonstrating that activated receptors bind etomidate more avidly than inactive receptors. The experimental PC_{50} values are remarkably close to, and therefore validate MWC model predictions for etomidate dissociation constants in both inactive and active receptors. Our results support MWC models as valid frameworks for understanding agonism, co-agonism, and modulation of ligand-gated ion channels.

Introduction

Functional models of ligand binding and efficacy at receptors such as ligand-gated ion channels incorporate the proposition that agonism is a feature of ligands that bind with higher affinity to active receptors relative to inactive receptors, and therefore shift the inactive⇔active equilibrium toward active (Auerbach, 2012; Buxton, 2006; Colquhoun, 1998; Kenakin, 2004). This concept applies to both orthosteric and allosteric agonists. Consequently, the apparent affinity of an agonist for receptors in assays of both function and ligand-binding depends on its intrinsic efficacy (Colquhoun, 1998). Monod-Wyman-Changeux (MWC) allosteric models of receptor function define agonist efficacy as the ratio of affinities for active versus inactive states (Changeux, 2012), and provide a framework for estimating agonist affinity and intrinsic efficacy parameters in ligand-gated ion channels, which are the only receptors where signals directly proportional to receptor activity (voltage-clamped currents) can be readily obtained (Auerbach, 2012; Chang and Weiss, 1999; Galzi et al., 1996; Rüsch et al., 2012; Rüsch et al., 2004). Nonetheless, experimental validation of model-derived estimates for agonist binding affinities at inactive receptors is confounded by agonist induction of receptor activation, which simultaneously alters agonist-receptor interactions. One rare example of this achievement used complex rapid mixing and fluorescent detection of the nicotinic agonist dansyl-C6-choline binding to *Torpedo* nicotinic acetylcholine receptors (Raines and Krishnan, 1998). In the present study, we identified a mutant γ-aminobutyric acid type A (GABA$_A$) receptor with unique functional characteristics that enable experimental determination of binding site occupancy for an allosteric agonist/modulator, etomidate, in both inactive and active receptors.

Synaptic GABA$_A$ receptors are pentameric membrane complexes typically formed from two α, two β, and one γ subunit symmetrically surrounding a chloride-conducting ion channel (Olsen and Sieghart, 2008). Each subunit contains a large N-terminal extracellular domain and four transmembrane domains (M1 to M4), with M2 domains from each subunit surrounding the

ion channel. The M1, M3, and M4 domains form an outer ring of helical domains between the M2 domains and membrane lipids. Two GABA sites per receptor are formed at the extracellular interfaces between α and β subunits.

The allosteric agonist used in this study is etomidate, a potent general anesthetic that acts by modulating GABA$_A$ receptors. In wild-type $\alpha1\beta2\gamma2L$ GABA$_A$ receptors, low etomidate concentrations enhance GABA-mediated receptor activation, while high etomidate concentrations ($\geq 10\ \mu M$) directly activate receptors in the absence of GABA. The gating effects of both GABA and etomidate are quantitatively described by a Monod-Wyman-Changeux (MWC) two-state allosteric co-agonist mechanism with two equivalent sites for etomidate (Guitchounts et al., 2012; Rüsch et al., 2004). The etomidate sites are located within transmembrane interfaces between α-M1 and β-M3 domains, based on labeling with photo-reactive etomidate derivatives (Chiara et al., 2011; Li et al., 2006).

The receptors we used in this study incorporate cysteine mutations at one photolabeled residue in etomidate binding sites: $\beta2$M286. Studies in rat $\alpha1\beta2$M286C$\gamma2L$ GABA$_A$ receptors demonstrate that the $\beta2$M286C sulfhydryl is covalently modified by a water-soluble reagent, p-choromercuribenzene sulfonate (pCMBS), and that GABA activation accelerates this reaction (Bali and Akabas, 2004; Bali and Akabas, 2012). We conducted a detailed electrophysiological analysis of heterologously expressed human $\alpha1\beta2$M286C$\gamma2L$ GABA$_A$ receptor function, which revealed the absence of etomidate agonism. However, etomidate modulation of GABA-mediated activation is maintained in the mutant receptors, albeit weaker than in wild-type. These properties allowed us to experimentally determine etomidate affinity in both inactive and GABA-activated mutant channels, based on etomidate-dependent inhibition of covalent bond formation between $\beta2$M286C and pCMBS. By tracking the electrophysiological effects of this reaction in mutant receptors, we quantified the apparent rate of pCMBS-$\beta2$M286C bond formation in both inactive (no GABA) and GABA-activated receptors, while varying etomidate

concentration. High concentrations of etomidate completely protected β2M286C from covalent

modification. Etomidate-dependent receptor occupancy estimates based on cysteine protection

studies were compared to those predicted by fitting functional data with the MWC allosteric co-

agonist model for etomidate and GABA (Rüsch et al., 2004).

Materials and Methods

Animal use: Female *Xenopus laevis* were housed in a veterinary-supervised environment in accordance with local and federal guidelines. Frogs were anesthetized by immersion in 0.2% tricaine (Sigma-Aldrich, St. Louis, MO) prior to mini-laparotomy to harvest oocytes.

Chemicals: R(+)-Etomidate was obtained from Bedford Laboratories (Bedford, OH). The clinical preparation in 35% propylene glycol was diluted directly into buffer. Previous studies have shown that propylene glycol at the dilutions used for these studies has no effect on GABA$_A$ receptor function (Rüsch et al., 2004). Picrotoxin (PTX) was purchased from Sigma-Aldrich (St. Louis, MO) and a 2mM solution in electrophysiology buffer was made by prolonged gentle shaking. Alphaxalone was purchased from MP Biomedical (Solon, OH) and prepared as a 2 mM stock solution in DMSO. During experiments with alphaxalone, DMSO was present at 0.1%, which had no effect on GABA$_A$ receptor function. *p*-Chloromercuribenzenesulfonic acid sodium salt (pCMBS) was purchased from Toronto Research Chemicals (North York, Ontario, Canada) and maintained in a cold dry environment. Fresh solutions of pCMBS were prepared frequently and sulfhydryl modifying activity was assayed using colorimetric titration of dithionitrobenzoic acid (DTNB), as described by Karlin & Akabas (1998).

Molecular Biology: cDNAs for human GABA$_A$ receptor α_1, β_2, and γ_{2L} subunits were cloned into pCDNA3.1 vectors (Invitrogen, Carlsbad, CA). The β2M286C mutation was created with oligonucleotide-directed mutagenesis using a QuikChange kit (Stratagene, La Jolla, CA). Clones from the mutagenesis reaction were subjected to DNA sequencing through the entire cDNA region to confirm the presence of the mutation and absence of stray mutations.

Oocyte Electrophysiology: Messenger RNA synthesis and *Xenopus* oocyte expression were performed as previously described (Stewart et al., 2008). Experiments were performed at room temperature (21-23 °C) in ND96 buffer (in mM: 96 NaCl, 2 KCl, 0.8 MgCl$_2$, 1.8 CaCl$_2$, 5 HEPES, pH 7.5). GABA$_A$ receptor responses to GABA were assessed in *Xenopus* oocytes

using two microelectrode voltage clamp electrophysiology, as previously described (Rüsch et al., 2004). GABA pulses were from 5 to 20s, depending on the concentration of GABA used and the time to peak current. Normalizing GABA responses at maximal GABA (2-10 mM), were recorded every 2nd or 3rd sweep. Oocyte currents were low-pass filtered at 1 kHz (Model OC-725B, Warner Instruments, Hamden, CT) and digitized at 2 kHz using commercial digitizer hardware (Digidata 1200, Molecular Devices, Sunnyvale, CA) and software (Clampex 7, Molecular Devices) for off-line analysis.

   Cysteine Modification with pCMBS and Etomidate Protection in Xenopus Oocytes. The pCMBS concentrations were chosen so that control modification (with or without 2 mM GABA) appeared complete after 40-60 s of pCMBS exposure. In modification experiments, GABA responses to both low GABA (30 μM, approx. EC$_5$) and high GABA (1-2 mM) were measured before and after each exposure to pCMBS ± GABA. Additional control modification experiments included 2 μM alphaxalone with GABA in order to maximize the fraction of activated receptors. In protection experiments, etomidate was present throughout the experiment, and was thus added to background buffer, pCMBS solutions, and GABA solutions. Because etomidate enhances GABA responses in the mutant receptors, functional testing after modification was performed with etomidate plus low GABA (combined efficacy about 5% of maximum) and etomidate plus 1 mM GABA. In most experiments, modification exposures to pCMBS of 5-10s each were performed, followed by at least two minutes of wash for pCMBS alone and longer washes (5 to 10 min) when GABA and/or etomidate was present. Up to ten modification and post-test cycles were performed on each oocyte. The ratio of low GABA vs. high GABA current responses was calculated, and all ratios were normalized to the control ratio before pCMBS exposure.

   Normalized response ratios were plotted as a function of total pCMBS exposure (seconds or seconds × [pCMBS]). For some data sets, exponential time constants were derived from single

exponential fits to data. Initial modification rates were also calculated as slopes ($M^{-1}s^{-1}$) of linear least squares fits to the initial three or four normalized ratio points (baseline and two or three post-modification points).

Electrophysiology in HEK293 Cell Membrane Patches: HEK293 cell maintenance and transfection for functional studies were performed as previously described (Scheller and Forman, 2002). Cells transfected with plasmids encoding $GABA_A$ receptor subunits were maintained in culture medium for 24-48 hours prior to electrophysiology experiments. Current recordings from excised outside-out membrane patches were performed at room temperature (21-23 °C) under –50 mV voltage-clamp as previously described (Scheller and Forman, 2002). Bath and superfusion solutions contained (in mM) 145 NaCl, 5 KCl, 10 HEPES, 2 $CaCl_2$, and 1 $MgCl_2$ at pH 7.4 (pH adjusted with N-methyl glucosamine). The intracellular (pipette) fluid contained (in mM) 140 KCl, 10 HEPES, 1 EGTA, and 2 $MgCl_2$ at pH 7.3 (pH adjusted with KOH). Currents were stimulated using pulses of GABA delivered via a quad (2×2) superfusion pipette coupled to piezo-electric elements that switched superfusion solutions in under 1 ms. Currents were filtered at 5 kHz and digitized at 10 kHz for off-line analysis.

Data Analysis: Quantitative analyses of agonist concentration-responses, etomidate-induced left shift, and allosteric co-agonist model fitting followed our approach described elsewhere (Desai et al., 2009; Stewart et al., 2008). Agonist (GABA or etomidate) concentration-response data were fitted with logistic functions using non-linear least-squares (Origin 6.1, OriginLab, Northampton, MA and Graphpad Prism 5.0, Graphpad Software, La Jolla, CA):

$$\frac{I}{I_{max}^{GABA}} = Max \times \frac{[Agonist]^{nH}}{[Agonist]^{nH} + EC_{50}{}^{nH}} \qquad \text{Eq. 1}$$

where nH is Hill slope.

Etomidate left-shift values were calculated as the ratio of the GABA EC_{50} values in the absence of drug to that in the presence of 3.2 μM drug. Large EC_{50} ratios indicate strong modulation, while a ratio of 1.0 or less indicates no positive modulation.

Etomidate-dependent effects on pCMBS modification (protection analysis) were also analyzed by non-linear least-squares fits to a logistic function with nH fixed at 1.0 and the minimum modification rate fixed at zero (based on results with high [etomidate]). We defined the PC_{50} as the etomidate concentration resulting in 50% reduction in the maximum modification rate.

PTX-sensitive leak currents (I_{PTX}) normalized to I_{max}^{GABA} were measured to help estimate basal open probability (P_0). P_0 was assessed in both $\alpha 1\beta 2M286C\gamma 2L$ receptors and in double-mutant $\alpha 1L264T\beta 2M286C\gamma 2L$ receptors. The $\alpha 1L264T$ mutation confers spontaneous gating to the double mutant for comparison with $\alpha 1L264T\beta 2\gamma 2L$, which we have described previously (Rüsch et al., 2004). Maximal GABA efficacy was estimated using a single sweep protocol with 2 μM alphaxalone as allosteric enhancer (Desai et al., 2009). If addition of alphaxalone increases current beyond that elicited with maximal GABA alone, then GABA is not opening all activatable channels.

Estimated open probability (P_{open}^{est}) was calculated by explicitly adding average spontaneous activity ($\frac{I_{PTX}}{I_{max}^{GABA}}$) to normalized activated current ($\frac{I}{I_{max}^{GABA}}$) and renormalizing to the full range of open probability, bracketed by alphaxalone enhanced current ($\frac{I^{GABA+Alphax}}{I_{max}^{GABA}}$; $P_{open} = 1.0$) and picrotoxin-blocked basal current ($P_{open} = 0$):

$$P_{open}^{est} = \frac{\dfrac{I}{I_{max}^{GABA}} + \dfrac{I_{PTX}}{I_{max}^{GABA}}}{\dfrac{I^{GABA+Alphax}}{I_{max}^{GABA}} + \dfrac{I_{PTX}}{I_{max}^{GABA}}} \qquad \text{Eq. 2}$$

MOL #84558

Non-linear least squares fits to a Monod-Wyman-Changeux two-state co-agonist mechanism (Eq. 3) used P_{open}^{est} data (Eq. 2) from GABA concentration-responses (with and without etomidate) and etomidate-dependent activation (with and without EC5 GABA). Both [GABA] and [ETO] were independent variables:

$$P_{open} = \frac{1}{1 + L_0 \left(\frac{1 + [GABA]/K_G}{1 + [GABA]/cK_G} \right)^2 \left(\frac{1 + [ETO]/K_E}{1 + [ETO]/dK_E} \right)^2}$$

Eq. 3

L_0 in Eq. 3 is a dimensionless basal equilibrium gating variable, approximately P_0^{-1}. Spontaneous activity was undetectable in $\alpha 1 \beta 2 M286C \gamma 2L$ receptors. Therefore, we constrained L_0 to a value based on previous estimates for wild-type L_0 (25,000), corrected for the relative spontaneous activity of receptors with the $\alpha 1 L264T$ mutations in wild-type vs. $\beta 2 M286C$ backgrounds. The ratio of spontaneous open probabilities in these receptors is approximately 3 (see results), so we constrained L_0 to a value of 75,000 for $\alpha 1 \beta 2 M286C \gamma 2L$ receptors. K_G and K_E are equilibrium dissociation constants for GABA and etomidate binding to inactive receptors, and c and d are dimensionless parameters representing the respective ratios of dissociation constants in active versus inactive states. The intrinsic agonist efficacies of GABA and etomidate are inversely related to, respectively, c and d.

Analysis of patch macrocurrents for activation, desensitization, and deactivation kinetics was performed as described in Scheller & Forman (2002) using non-linear least squares fits to Eq. 4 and F-tests at P = 0.99 (Clampfit8.0; Molecular Devices) to choose the best number of exponents:

$I(t) = A_1 \times exp(-t/\tau_1) + A_2 \times exp(-t/\tau_2) + A_3 \times exp(-t/\tau_3) + C$ Eq. 4

Activation traces were fitted best with a single exponent, while desensitization and deactivation were fitted best with two exponents.

Statistical Analysis: Results are reported as mean ± standard deviation. Nonlinear regression errors are those from fits in Origin 6.1 (OriginLab), GraphPad Prism 5.02 (Graphpad,

11

MOL #84558

Software) or Clampfit 8.0 (Molecular Devices). Statistical comparison of fitted parameters was

performed using Prism 5.02. Statistical significance was inferred at $p < 0.05$.

12

Results

Functional characterization of $\alpha1\beta2M286C\gamma2L$ GABA$_A$ receptors: Voltage-clamped

oocytes expressing $\alpha1\beta2M286C\gamma2L$ receptors produced inward currents in response to GABA

(Fig 1A). Etomidate (3.2 μM) enhanced responses at all GABA concentrations (Fig 1B). A

logistic fit to pooled concentration-response data (Fig 1C, solid squares; n $\geq$ 6) resulted in a

GABA EC$_{50}$ for this mutant of 180 μM, while the average EC$_{50}$ from independent analyses of six

separate oocytes with complete data sets was 210 μM (Table 1). These values are about six-

fold higher than the wild-type GABA EC$_{50}$ (Table 1). In the presence of 3.2 μM etomidate,

GABA concentration responses shift leftward (Fig. 1C, open squares), reducing GABA EC$_{50}$ two

to three-fold. This is a significantly smaller leftward-shift ratio than that observed in $\alpha1\beta2\gamma2L$

receptors in the presence of 3.2 μM etomidate (Table 1).

Etomidate at up to 1 mM elicited no significant direct activation of $\alpha1\beta2M286C\gamma2L$ receptors

(< 1.5% of maximal GABA currents; Fig 1D). We also studied etomidate-dependent modulation

of low GABA (20 μM $\approx$ EC$_3$) currents. Modulation of low GABA responses was characterized by

an etomidate EC$_{50}$ of 24 μM and maximal enhancement at an etomidate concentration of 100

μM resulted in current responses averaging about 70% of maximal GABA currents (Fig 1D).

Rapid superfusion and patch-clamp electrophysiology was used to study macro-current

kinetics of $\alpha1\beta2M286C\gamma2L$ receptors. Rapid application of 10 mM GABA to outside-out

membrane patches from HEK293 cells expressing $\alpha1\beta2M286C\gamma2L$ receptors resulted in

currents with kinetic properties similar to those recorded with wild-type receptors (Fig 1E, Table

1). The maximal current activation rate was approximately 3000 s^{-1}, desensitization proceeds

with two rates, and deactivation also displayed two distinct rates.

Allosteric modeling of $\alpha1\beta2M286C\gamma2L$ GABA$_A$ receptor function. Quantitative analysis

with the allosteric co-agonist model (Fig. 2A) requires transformation of concentration-response

data into estimates of open probability, which in turn is dependent on estimates of maximal

GABA efficacy and spontaneous receptor activity. Alphaxalone, which does not interact with

etomidate sites (Li et al., 2010), enhances maximal (3 mM) GABA currents by more than 50%,

resulting in an estimated GABA efficacy of 0.64 (Fig 2B). Picrotoxin-sensitive spontaneous

activity was not detected in cells expressing α1β2M286Cγ2L receptors (Fig 2C), so no P_{open}

correction was needed for spontaneous activity. Estimated P_{open} values for averaged GABA-

concentration responses (with and without etomidate) and etomidate-dependent modulation of

GABA EC_5 responses were calculated using Eq. 2 (methods).

Based on previously published experiments, the basal gating parameter, L_0, for wild-type

α1β2γ2L is estimated to be around 25,000 (Desai et al., 2009; Rüsch et al., 2004). In double-

mutant α1L264Tβ2M286Cγ2L receptors, picrotoxin-sensitive spontaneous activity averaged 3%

of the maximal GABA-activated currents (Fig 2D). In comparison, oocyte-expressed

α1L264Tβ2γ2L receptors display about 10% spontaneous activation (Desai et al., 2009; Rüsch

et al., 2004). Assuming that the basal gating effects of α1L264T and β2M286C are independent,

the β2M286C mutation reduces spontaneous activation around three-fold, so we set the value

of L_0 for α1β2M286Cγ2L receptors in global analysis at 75,000, three times that of wild-type.

With L_0 thus constrained, the averaged P_{open}^{est} values for α1β2M286Cγ2L resulted in a good

overall fit to the MWC co-agonist model (Eq. 3 in Methods; R^2 = 0.98), which is illustrated in Figs

2E and 2F. The fitted parameters are reported in Table 1. The fitted estimate for GABA affinity

in inactive α1β2M286Cγ2L receptors ($K_G \approx$ 270 μM) is higher than those in wild-type models (60

to 90 μM), while fitted GABA efficacy ($c^{-1} \approx$ 420) is not far from previous estimates for wild-type

($c^{-1} \approx$ 530 to 590). The fitted etomidate dissociation constant ($K_E \approx$ 12 μM) is lower than prior

estimates in wild-type (20 to 40 μM), while the largest difference between wild-type and

α1β2M286Cγ2L models is the etomidate efficacy parameter ($d^{-1} \approx$ 8.5 in the β2M286C mutant

model versus $d^{-1} \approx$ 104 to 130 in wild-type models).

14

PCMBS modification of $\alpha 1\beta 2M286C\gamma 2L$ receptors. PCMBS exposure resulted in
irreversible functional effects on $\alpha 1\beta 2M286C\gamma 2L$ receptors, both in the absence and presence
of GABA (Fig 3). Receptors exposed to pCMBS developed larger current responses to low
GABA concentrations (30 μM, approx EC$_5$) relative to high GABA concentrations (1-2 mM).
Exposure to 50 μM pCMBS in the absence of GABA (inactive receptors) resulted in $I_{30\mu M}/I_{2mM}$
increasing to about double its baseline value (Fig 3A, B) in 60 to 80 seconds. Exponential fits to
normalized $I_{30\mu M}/I_{2mM}$ as a function of pCMBS exposure time indicated modification rates
averaging 1000 ± 470 M^{-1}s^{-1} (mean $\pm$ SD, n = 4). When receptors were exposed to pCMBS co-
applied with 2 mM GABA, the apparent rate of receptor modification increased (Fig 3C, D).
Exponential fits indicated rates of 1800 ± 580 M^{-1}s^{-1} (mean $\pm$ SD, n = 4). In addition, the
amplitude of the pCMBS-induced gating effect was consistently larger when GABA was present
(averaging six-fold enhancement above baseline).

To examine the impact of GABA in more detail, we performed experiments where
$\alpha 1\beta 2M286C\gamma 2L$ receptors were first modified with 50 μM pCMBS in the absence of GABA, then
exposed to GABA + pCMBS. These studies reveal that addition of GABA to pCMBS increases
the response to low GABA ($I_{30\mu M}$; Fig 3E, triangles) beyond that observed after pCMBS alone.
Moreover, the pCMBS-induced response to high GABA (I_{2mM}; Fig 3E, diamonds) drops far more
following GABA + pCMBS exposure than with pCMBS alone. Together these effects combine
to increase the $I_{30\mu M}/I_{2mM}$ ratio when GABA is present beyond the level achieved with pCMBS
alone (Fig 3F). Exposure to higher (250-500 μM) pCMBS also resulted in higher (three to four-
fold) $I_{30\mu M}/I_{2mM}$ ratios (data not shown). These results suggest that partial modification of
$\beta 2M286C$ was achieved with 50 μM pCMBS alone, and that modification in the presence of
GABA results in accumulation of deeply desensitized receptors that did not re-activate on the
timescale of our experiments.

15

Because GABA affected the change in amplitude of $I_{30\mu M}/I_{2mM}$ after pCMBS more than the apparent exponential rate change, we adopted an alternative approach to estimating initial rates of pCMBS modification, using linear slope analysis. Slope analyses resulted in average initial modification rates of around 400 $M^{-1}s^{-1}$ in the absence of GABA and 11000 $M^{-1}s^{-1}$ in the presence of GABA. This suggests that GABA activation increases pCMBS modification rates over 20-fold, a much larger ratio than that based on exponential rate analysis (1.8-fold).

Control experiments in $\alpha1\beta2\gamma2L$ receptors exposed to pCMBS (up to 2 mM for 60 s) failed to demonstrate significant (> 10%) functional change in electrophysiological responses to zero, low or high GABA (data not shown).

Etomidate protection at $\alpha1\beta2M286C\gamma2L$ receptors

For etomidate protection experiments, receptors were equilibrated with etomidate before and during pCMBS modification and post-modification functional testing. Because etomidate enhances responses to low GABA more than high GABA, we reduced the low GABA concentration used for post-modification testing (1-10 μM) to produce about 5% maximal response in the presence of etomidate. Initial modification rates were quantified from linear fits to normalized I_{loGABA}/I_{1-2mM} ratios after two or three pCMBS exposures.

In the absence of GABA, initial slope analysis resulted in an apparent $\beta2M286C$ modification rate of 400 ± 96 $M^{-1}s^{-1}$ (Fig. 4A, red squares). Addition of 300 μM etomidate completely inhibited pCMBS modification (initial slope $\leq$ 0; Fig 4A, brown diamonds). We also measured the initial rate of pCMBS modification at $\beta2M286C$ in the presence of etomidate concentrations ranging from 3 to 100 μM. Data for 3 μM and 30 μM etomidate are shown in Fig. 4A. The modification rate vs. [etomidate] data were fit by non-linear least-squares to a logistic function with nH = 1, resulting in an estimate of 14 μM for the 50% protecting concentration (PC_{50}; Fig. 4B).

In the presence of GABA (2 mM), initial slope analysis revealed an apparent β2M286C modification rate of 11,300 ± 2000 $M^{-1}s^{-1}$ (Fig 4C, red squares). Addition of alphaxalone (2 μM) to GABA further increased the apparent initial rate of β2M286C modification to 16,600 ± 4000 $M^{-1}s^{-1}$ (Fig 4C, green half-filled hexagons). In contrast, addition of etomidate (range 1 to 300 μM) reduced initial rates of GABA-activated α1β2M286Cγ2L receptor modification by pCMBS. Figure 4C displays data in the presence of 3, 30, and 300 μM etomidate. Logistic analysis of modification rates using the control with GABA alone results in a fitted etomidate PC_{50} value of 2.2 μM for GABA-activated receptors (Fig. 4D, solid black line). Substituting the control modification rate measured with alphaxalone plus GABA (closer to 100% open receptors) results in a leftward shift of the logistic fit, with PC_{50} = 1.1 μM (Fig 4D, dashed black line).

17

Discussion

The major finding of this study is that GABA$_A$ receptor activation results in increased affinity for the allosteric agonist etomidate. While state-dependent binding is inherent in theoretical models of receptor agonism, and resting-state affinity may sometimes be inferred from functional analysis, direct measurement of agonist occupation in inactive receptors represents an experimental challenge. In this study, we assessed rates of pCMBS modification at cysteine-substituted β2M286 residues to estimate etomidate occupancy at its GABA$_A$ receptor binding sites.

The substituted cysteine accessibility method (SCAM) provides tools for probing the proximity of ligands and specific receptor residues. SCAM coupled with ligand protection has been used in heterologously expressed GABA$_A$ receptors to map residues in orthosteric agonist (GABA) sites (Wagner and Czajkowski, 2001) and transmembrane sites for propofol (Bali and Akabas, 2004). Our approach assumed that etomidate sterically hinders the formation of a covalent bond between pCMBS and the β2M286C sulfhydryl. Thus, as etomidate occupies an increasing fraction of its sites, the rate of covalent modification should drop from the control value. Etomidate site occupancy depends on its concentration and binding affinity. Other factors that could influence sulfhydryl modification rates include altering local pCMBS concentration, sulfhydryl ionization, and availability of water, which participates in covalent bond formation (Karlin and Akabas, 1998). Such factors may also change with the receptor's functional state. Thus, to isolate the steric effects of ligand binding, other investigators using SCAM protection have established roughly equivalent mixes of receptor states in control modification and protection experiments (Bali and Akabas, 2004). Because of the unique features of the α1β2M286Cγ2L receptor, we were able to study etomidate protection under two conditions where essentially all receptors were in either 1) the inactive state or 2) the GABA-activated state.

Functional characterization of $\alpha1\beta2M286C\gamma2L$ receptors revealed a number of important changes from wild-type $\alpha1\beta2\gamma2L$ (Table 1). The $\alpha1\beta2M286C\gamma2L$ receptors are characterized by a high GABA EC_{50} and reduced apparent GABA efficacy. In addition, direct etomidate agonism was absent in $\alpha1\beta2M286C\gamma2L$ receptors. The reduced efficacy of both GABA and etomidate are partially explained by reduced spontaneous gating in the mutant receptors, which was evident in mutant-cycle experiments combining $\beta2M286C$ with a spontaneous activation mutation, $\alpha1L264T$ (Fig 2D). Etomidate modulation was also significantly diminished in $\alpha1\beta2M286C\gamma2L$ receptors. Indeed, MWC coagonist model analysis (Fig 2, Table 1) suggests that the mutation reduces the agonist efficacy of etomidate, but not of GABA. The etomidate efficacy parameter (d^{-1}) for the mutant receptors is 8.5, while estimates for wild-type receptors are between 100 and 130 (Desai et al., 2009; Rüsch et al., 2004; Stewart et al., 2008), a 12 to 15-fold difference in gating effect per etomidate site. Etomidate's maximal agonist efficacy can be calculated from Eq. 3 (methods) as $(1 + L_0d^2)^{-1}$. Using values from Table 1, etomidate activates 41% of wild-type and 0.09% of $\alpha1\beta2M286C\gamma2L$ receptors. Nonetheless, etomidate efficacy is sufficient to produce positive modulation of GABA-induced activation in the mutant channels (Fig 1D).

Interestingly, some functional effects of the $\beta2M286C$ mutation are opposite of those seen with the $\beta2M286W$ mutation, which increases spontaneous activation, and sensitizes receptors to agonism by GABA (Stewart et al., 2008). However, both tryptophan and cysteine mutations at $\beta2M286$ reduce etomidate modulation and etomidate direct activation in comparison to wild-type. Investigation of various $\beta M286$ mutations demonstrated that side-chain volume may be an important determinant of propofol effects (Krasowski et al., 2001). Our results show that the $\beta M286$ side-chain influences both anesthetic binding and basal channel gating, and that the magnitude and directions of these effects are independent.

As previously reported for rat $GABA_A$ receptors (Bali and Akabas, 2004; Bali et al., 2009), we found that in human receptors, $\beta2M286C$ is accessible to the water-soluble reagent pCMBS.

Thus, the β2M286 sidechain is located, at least part of the time, in a position where water permeates into the transmembrane domains of the receptor, and an aqueous pathway from the extracellular space probably exists. Acceleration by GABA of β2M286C modification also indicates that the configuration of the receptor structures near β2M286 changes with GABA binding.

The highest etomidate concentration tested (300 μM) fully blocked irreversible gating effects associated with pCMBS modification.   Complete etomidate protection most likely indicates an intimate steric relationship between the β2-286 residue and receptor-bound etomidate. The native β2M286 residue was photolabeled by both azi-etomidate and TDBzl-etomidate, supporting this inference. Nonetheless, because an ester linkage separates the photoreactive moieties of the photolabels from the hydrophobic core structures of etomidate, we cannot definitively conclude that the β2M286 sidechain is within the etomidate binding pocket, rather than just near it. An alternative mechanism is that etomidate blocks the aqueous pathway for pCMBS access. Bali and Akabas (2004) found that propofol also protects βM286C from modification in GABA-activated receptors. Propofol also inhibits azi-etomidate photolabeling (Li et al., 2010), although not completely. The most parsimonious interpretation is that both propofol and etomidate have partially overlapping binding sites that abut β2M286.

Etomidate occupancy of its sites, inferred from protection of β2M286C from pCMBS modification, is dependent on both the concentration of etomidate and on the receptor state. The PC$_{50}$ for etomidate protection in the resting state is 14 μM (Fig 4B), close to the α1β2M286Cγ2L resting state K$_E$ of 12 μM estimated from MWC allosteric model fitting. In the allosteric model, the estimated dissociation constant for etomidate binding to active α1β2M286Cγ2L receptors is K$_E$×d = 1.4 μM. This is within the range of PC$_{50}$ values (1.1 to 2.2 μM) derived from active-state protection experiments. Thus, both allosteric model analysis and protection experiments converge on similar affinity estimates, indicating that etomidate binds

about 10-fold more tightly to active than to inactive α1β2M286Cγ2L receptors. The active-state

PC$_{50}$ value closest to K$_E$ × d was obtained using the control modification rate in the presence of

alphaxalone, which increased the fraction of activated receptors without blocking pCMBS

access to the etomidate site. Indeed, taking into account both etomidate's positive gating

modulation and its protective action at β2M286C, the MWC coagonist model closely predicts

open-state protection results (Fig 4D, solid red line). These results validate the MWC allosteric

model and suggest that estimates for etomidate affinity and efficacy in wild-type GABA$_A$

receptors (Table 1) are reasonably accurate. More generally, this result is in accord with

theories of agonist-receptor interactions (Buxton, 2006).

The close match between etomidate PC$_{50}$ values and MWC model estimates for

microscopic dissociation constants is notable, because etomidate binding is reversible, while

pCMBS modification is irreversible. In protection experiments, we reduced systematic bias from

varying etomidate association rates at different concentrations by pre-equilibrating receptors

with etomidate. As long as etomidate binding and dissociation rates are fast compared to the

pCMBS reaction at β2M286C, a reasonable assumption under the conditions we selected, then

the observed rate of covalent bond formation should reflect the initial fraction of unoccupied

etomidate sites. Another potential source of divergence between our functional modeling and

protection results is receptor desensitization, which is not factored into the two-state MWC

model. Figure 1E shows that substantial desensitization of α1β2M286Cγ2L receptors occurs

within seconds after exposure to high GABA. The fact that open state etomidate affinity

estimates from equilibrium MWC modeling matches estimates from protection in a dynamic

mixture of open and desensitized receptors suggests that affinities for both open and

desensitized states are similar. This is consistent with observations that etomidate does not

alter GABA$_A$ receptor desensitization kinetics (Zhong et al., 2008). To test this idea, studies

comparing etomidate protection at β2M286C in open versus desensitized receptors will be

needed. Moreover, the fraction of desensitized receptors when GABA is absent is unknown and cannot be determined from functional studies, but the close match between K_E from functional modeling and PC_{50} in inactive receptors suggests that at most a small fraction of channels are in high-affinity states.

While thorough characterization of GABA and etomidate-dependent receptor activity provided us with a mechanistic framework to interpret multiple effects of the β2M286C mutation, the major factor influencing design and interpretation of SCAM protection experiments was the absence of etomidate agonism. Indeed, allosteric principles imply generally that in SCAM protection studies using ligands with agonist activity, the presence or absence of significant agonism in cysteine substituted mutant channels determines the conditions under which protection may be tested. In mutant channels that, like wild-type GABA$_A$ receptors, are efficaciously activated by etomidate, the GABA-activated open state is the only viable control condition for protection studies, and protection may be observed using low ligand concentrations predicted to occupy most high-affinity active-state receptors. With mutations like β2M286C, where etomidate efficacy is significantly weakened but not absent, open-state affinity is predicted to be only modestly higher than in inactive receptors, indicating the likely need for higher concentrations of the protective ligand, and also establishing the potential for state-dependent protection experiments. More specifically, absent etomidate agonism coupled with retained GABA agonism in α1β2M286Cγ2L channels enabled protection studies in two different states. Finally if a cysteine mutation eliminates both etomidate agonism and modulation of GABA-activated responses, then both active and resting state receptors are expected to display low affinities, requiring high etomidate concentrations to test for protection.

MOL #84558

Acknowledgments

Authorship Contributions

Participated in research design: Stewart, Forman

Conducted experiments: Stewart, Hotta, Desai

Performed data analysis: Stewart, Hotta, Forman, Desai

Wrote or contributed to writing of manuscript: Stewart, Forman

References

Auerbach A (2012) Thinking in cycles: MWC is a good model for acetylcholine receptor-channels. *J Physiol* **590**:93-98.

Bali M and Akabas MH (2004) Defining the propofol binding site location on the GABAA receptor. *Mol Pharmacol* **65**:68-76.

Bali M and Akabas MH (2012) Gating-induced Conformational Rearrangement of the gamma-Aminobutyric Acid Type A Receptor beta-alpha Subunit Interface in the Membrane-spanning Domain. *J Biol Chem* **287**:27762-27770.

Bali M, Jansen M and Akabas MH (2009) GABA-induced intersubunit conformational movement in the GABAA receptor alpha1M1-beta2M3 transmembrane subunit interface: Experimental basis for homology modeling of an intravenous anesthetic binding site. *J Neurosci* **29**:3083-3092.

Buxton ILO (2006) Chapter 1: Pharmacokinetics and Pharmacodynamics, in *Goodman & Gilman's The Pharmacological Basis of Therapeutics*, 11th ed (Brunton LL, Lazo JS and Parker KL eds) pp 1-39, McGraw-Hill, New York, NY, USA.

Chang Y and Weiss DS (1999) Allosteric activation mechanism of the alpha1beta2gamma2 gamma-aminobutyric acid type A receptor revealed by mutation of the conserved M2 leucine. *Biophys J* **77**:2542-2551.

Changeux JP (2012) Allostery and the Monod-Wyman-Changeux model after 50 years. *Annu Rev Biophys* **41**:103-133.

Chiara DC, Dostalova Z, Jayakar SS, Zhou X, Miller KW and Cohen JB (2011) Mapping general anesthetic binding site(s) in human alpha1beta3 gamma-aminobutyric acid type A receptors with [(3)H]TDBzl-etomidate, a photoreactive etomidate analogue. *Biochemistry* **51**:836-847.

Colquhoun D (1998) Binding, gating, affinity and efficacy: the interpretation of structure-activity relationships for agonists and of the effects of mutating receptors. *Br J Pharmacol* **125**:924-947.

Desai R, Rüsch D and Forman SA (2009) Gamma-amino butyric acid type A receptor mutations at beta2N265 alter etomidate efficacy while preserving basal and agonist-dependent activity. *Anesthesiology* **111**:774-784.

Galzi JL, Edelstein SJ and Changeux J (1996) The multiple phenotypes of allosteric receptor mutants. *Proc Natl Acad Sci U S A* **93**:1853-1858.

Guitchounts G, Stewart DS and Forman SA (2012) The Two Etomidate Sites in alpha1beta2gamma2 gamma-Aminobutyric Acid Type A Receptors Contribute Equally and Noncooperatively to Modulation of Channel Gating. *Anesthesiology* **116**:1235-1244.

Karlin A and Akabas MH (1998) Substituted-cysteine accessibility method. *Meth Enzymol* **293**:123-145.

Kenakin T (2004) Principles: receptor theory in pharmacology. *Trends Pharmacol Sci* **25**:186-192.

Krasowski MD, Nishikawa K, Nikolaeva N, Lin A and Harrison NL (2001) Methionine 286 in transmembrane domain 3 of the GABAA receptor beta subunit controls a binding cavity for propofol and other alkylphenol general anesthetics. *Neuropharmacology* **41**:952-964.

Li GD, Chiara DC, Cohen JB and Olsen RW (2010) Numerous classes of general anesthetics inhibit etomidate binding to gamma-aminobutyric acid type A (GABAA) receptors. *J Biol Chem* **285**:8615-8620.

Li GD, Chiara DC, Sawyer GW, Husain SS, Olsen RW and Cohen JB (2006) Identification of a GABA$_A$ receptor anesthetic binding site at subunit interfaces by photolabeling with an etomidate analog. *J Neurosci* **26**:11599-11605.

Olsen RW and Sieghart W (2008) International Union of Pharmacology. LXX. Subtypes of gamma-aminobutyric acid(A) receptors: Classification on the basis of subunit composition, pharmacology, and function. *Pharmacol Rev* **60**:243-260.

Raines DE and Krishnan NS (1998) Transient low-affinity agonist binding to Torpedo postsynaptic membranes resolved by using sequential mixing stopped-flow fluorescence spectroscopy. *Biochemistry* **37**:956-964.

Rüsch D, Neumann E, Wulf H and Forman SA (2012) An Allosteric Coagonist Model for Propofol Effects on alpha1beta2gamma2L gamma-Aminobutyric Acid Type A Receptors. *Anesthesiology* **116**:47-55.

Rüsch D, Zhong H and Forman SA (2004) Gating allosterism at a single class of etomidate sites on alpha1beta2gamma2L GABA-A receptors accounts for both direct activation and agonist modulation. *J Biol Chem* **279**:20982-20992.

Scheller M and Forman SA (2002) Coupled and uncoupled gating and desensitization effects by pore domain mutations in GABA(A) receptors. *J Neurosci* **22**:8411-8421.

Stewart DS, Desai R, Cheng Q, Liu A and Forman SA (2008) Tryptophan mutations at azi-etomidate photo-incorporation sites on α1 or β2 subunits enhance GABAA receptor gating and reduce etomidate modulation *Mol Pharmacol* **74**:1687-1695.

Wagner DA and Czajkowski C (2001) Structure and dynamics of the GABA binding pocket: A narrowing cleft that constricts during activation. *J Neurosci* **21**:67-74.

Zhong H, Rusch D and Forman SA (2008) Photo-activated azi-etomidate, a general anesthetic photolabel, irreversibly enhances gating and desensitization of gamma-aminobutyric acid type A receptors. *Anesthesiology* **108**:103-112.

26

Footnotes

b) Part of this work was presented in an abstract (Poster 228.20) at the 57th Biophysical Society

Annual Meeting (February 2-6, 2013, Philadelphia, PA).

c) Reprint requests should be addressed to Stuart A. Forman, Dept. of Anesthesia Critical Care

& Pain Medicine, Jackson 444, Mass. General Hospital, 55 Fruit Street, Boston, 02114, USA.

Email: saforman@partners.org.

Legends for Figures

Figure 1: GABA Activation and Etomidate Modulation of $\alpha 1\beta 2$M286Cγ2L GABA$_A$

Receptors. **A)** Current traces are from a single Xenopus oocyte expressing $\alpha 1\beta 2$M286Cγ2L

receptors, activated with different GABA concentrations. GABA application (labeled in

micromolar) is indicated by horizontal bars above traces. **B)** Current traces are from the same

oocyte in panel A, stimulated with variable GABA (labeled in micromolar above panel A traces)

plus 3.2 μM etomidate. GABA and etomidate application is indicated by horizontal bars above

traces. **C)** Averaged ($\pm$ sd; n $\geq$ 6) GABA responses in the absence (solid squares) and

presence of etomidate (3.2 μM; open squares) are shown. Current responses were normalized

to the 3 mM GABA response in the same oocyte before averaging data from all cells. Lines

represent logistic fits (Eq. 1, methods) to data. Fitted parameters for GABA alone (solid line)

are $EC_{50} = 180 \pm 19$ μM and Hill slope = 1.3 + 0.16. Fitted parameters for GABA plus etomidate

(dashed line), are maximum = 1.44 + 0.04, $EC_{50} = 87 \pm 11$, and Hill slope = 1.5 $\pm$ 0.24.

Restricting analyses to data below 3 mM GABA does not alter the relative maxima or GABA

EC_{50} values. **D)** Average (+ sd; n $\geq$ 3) responses to etomidate alone (solid circles and line) or

to etomidate combined with 20 μM GABA (EC3; open circles). Currents were normalized to 3

mM GABA responses in the same oocyte before averaging. Etomidate direct activation was

never greater than 1.5% of maximal GABA response and was not further analyzed. The dashed

line through GABA EC3 enhancement data represents a logistic fit: maximum = 67 $\pm$ 5.0%, EC_{50}

= 24 $\pm$ 4.9 μM, Hill slope = 2.0 $\pm$ 0.75. **E)** A voltage-clamp current trace recorded from an

outside-out patch excised from an HEK293 cell expressing $\alpha 1\beta 2$M286Cγ2L receptors and

activated with 3 mM GABA for 1 s (bar above trace) delivered with sub-millisecond solution

switching. The trace displays rapid activation, biphasic desensitization, and biphasic

deactivation. Average rates for each phase are reported in Table 1.

Figure 2: Allosteric Co-agonist Modeling of GABA and Etomidate-Dependent Activity in $\alpha 1\beta 2M286C\gamma 2L$ GABA$_A$ Receptors. **A)** A schematic of the MWC equilibrium co-agonist mechanism for GABA and etomidate gating (Eq. 3 in methods). The mechanism is defined by five parameters: L_0 is a dimensionless basal equilibrium gating variable for inactive/active (R/O) receptors, which was constrained as described in the text. K_G and K_E are equilibrium dissociation constants for GABA and etomidate binding to inactive (R) receptors, and c and d are dimensionless parameters representing the ratios of dissociation constants in active (O) versus inactive (R) states. The agonist efficacies of GABA and etomidate are inversely related to, respectively, c and d. **B)** The trace depicts current recorded from a single oocyte expressing $\alpha 1\beta 2M286C\gamma 2L$ receptors, activated initially with 10 mM GABA, then with 10 mM GABA plus 2 μM alphaxalone, an allosteric modulator that does not interact directly with the etomidate site. Addition of alphaxalone increases the current elicited with GABA alone by about 50%, indicating that maximal GABA activates about 65% of receptors. **C)** Two current traces are shown, recorded from the same oocyte expressing $\alpha 1\beta 2M286C\gamma 2L$ receptors. 3 mM GABA activates a large inward current. Picrotoxin (PTX, 2 mM) does not produce any discernable outward current, indicating that the spontaneous open probability of receptors is below the threshold of detection (0.1%) with this method. **D)** Two current traces are shown, recorded from the same oocyte expressing $\alpha 1L264T\beta 2M286C\gamma 2L$ receptors. The $\alpha 1L264T$ mutation confers spontaneous activity, evident from the apparent outward current with picrotoxin application. The spontaneous activity is about 3% of the GABA-activated inward current. **E and F)** Symbols represent estimated P$_{open}$ values calculated from averaged data in Figure 1C and 1D. Lines through symbols represent fits to the MWC co-agonist model (Eq. 3, methods) with parameters reported in Table 1. Panel **E** shows GABA-dependent activation in the absence (solid squares) and presence of 3.2 μM etomidate (open squares). Panel **F** shows etomidate-dependent activation in the absence (solid circles) and presence of 20 μM GABA (open circles).

Figure 3: p-Chloromercuribenzene Sulfonate Modification of $\alpha1\beta2M286C\gamma2L$

GABA$_A$ Receptors is GABA-dependent. A) Traces represent currents recorded from a single

oocyte expressing $\alpha1\beta2M286C\gamma2L$ receptors, activated intermittently with 30 μM GABA

(horizontal bars above each trace), each scaled to normalizing 2 mM GABA responses (not

shown). Arrows indicate oocyte exposure to 50 μM pCMBS for 10 s (20 s for double arrows)

followed by wash. The $I_{30\mu M}$ approximately doubles relative to I_{2mM} after 60 seconds of pCMBS

exposure. **B)** Symbols represent the $I_{30\mu M}/I_{2mM}$ ratios from panel A normalized to the initial value

(t = 0), plotted against cumulative pCMBS exposure time. The solid line represents a single

exponential fit to the data, characterized by an exponential time constant of 27 ± 4.5 s (apparent

second-order reaction rate = 750 ± 130 $M^{-1}S^{-1}$). The dashed line is a linear fit to the first three

data points. Its slope is 0.0255 s^{-1}, resulting in an apparent initial reaction rate of 510 $M^{-1}s^{-1}$. **C)**

Current traces were recorded from another oocyte expressing $\alpha1\beta2M286C\gamma2L$ receptors,

activated intermittently with 30 μM and 2 mM GABA, each scaled to normalizing 2 mM GABA

responses (not shown). Starred arrows represent co-exposure to 50 μM pCMBS plus 2 mM

GABA for 5 seconds (10 s for double starred arrows) followed by wash. **D)** Symbols represent

$I_{30\mu M}/I_{2mM}$ ratios from panel C normalized to the initial value (t = 0), plotted against cumulative

exposure time. The $I_{30\mu M}/I_{2mM}$ ratio increases more than six-fold after 20 s of pCMBS/GABA

exposure. A single exponential fit results in a time constant of 8.3 ± 1.2 s (apparent second

order reaction rate = 2400 ± 340 $M^{-1}s^{-1}$). A linear fit to the first three data points results in a

slope of 0.454 s^{-1} (apparent initial rate = 9080 $M^{-1}s^{-1}$). **E)** Symbols represent peak currents

recorded from an oocyte expressing $\alpha1\beta2M286C\gamma2L$ receptors activated with either 30 μM

(triangles) or 2 mM (diamonds) GABA. The x-axis indicates cumulative exposure time to 50 μM

pCMBS in the absence of GABA (open symbols, up to 120 s), then in the presence of 50 μM

pCMBS plus 2 mM GABA (solid symbols). **F)** Symbols represent the $I_{30\mu M}/I_{2mM}$ ratios from data

in panel E, normalized to the initial value at t =0 (0.08).

Figure 4: Etomidate Inhibition of the β2M286C-pCMBS Reaction is Enhanced by

GABA. **A)** Symbols represent data from a subset of oocytes expressing α1β2M286Cγ2L

receptors used to study etomidate effects on pCMBS modification in the absence of GABA.

Normalized I_{loGABA}/I_{2mM} is plotted against cumulative pCMBS exposure (concentration × time).

Lines represent linear fits to all points in each data set: pCMBS alone = red squares (370 ± 14

$M^{-1}s^{-1}$; n = 6); pCMBS + 3 μM etomidate = orange triangles (260 ± 14 $M^{-1}s^{-1}$; n = 7); pCMBS +

30 μM etomidate = blue circles (54 ± 11 $M^{-1}s^{-1}$; n = 7); pCMBS + 300 μM etomidate = brown

diamonds (6 ± 8.5 $M^{-1}s^{-1}$; n = 4). **B)** Symbols represent the average (± sd) of initial rates of

pCMBS modification in the absence of GABA, from individual oocyte results, plotted against

[etomidate]. The line through data represents a logistic fit. Max = 400 ± 26 $M^{-1}s^{-1}$ and PC_{50} =

14.3 μM (95% CI = 7.5 to 27.2 μM). **C)** Symbols represent data from a subset of oocytes

expressing α1β2M286Cγ2L receptors used to study etomidate effects on pCMBS modification in

the presence of 2 mM GABA or GABA plus 2 μM alphaxalone. Normalized I_{loGABA}/I_{2mM} is plotted

against cumulative pCMBS exposure (concentration × time). Lines represent linear fits to all

points in each data set: GABA + pCMBS= red squares (11300 ± 580 $M^{-1}s^{-1}$; n = 5); GABA +

pCMBS + 3 μM etomidate = orange triangles (3500 ± 270 $M^{-1}s^{-1}$; n = 4); GABA + pCMBS + 30

μM etomidate = blue circles (600 ± 76 $M^{-1}s^{-1}$; n = 6); GABA + pCMBS + 300 μM etomidate =

brown diamonds (-40 ± 11 $M^{-1}s^{-1}$; n = 3); GABA + alphaxalone = green half-fill hexagons (16600

± 960 $M^{-1}s^{-1}$; n = 8). **D)** Open circles represent the average (± sd) of initial rates of pCMBS

modification in the presence of GABA, from individual oocyte results, plotted against [etomidate].

The solid line through data represents a logistic fit: Max = 11300 ± 490 $M^{-1}s^{-1}$ and PC_{50} = 2.2 μM

(95% CI = 1.5 to 3.1 μM). The dashed line represents a logistic fit using the GABA +

alphaxalone control: Max = 16600 ± 890 $M^{-1}s^{-1}$ and PC_{50} = 1.1 µM (95% CI = 0.65 to 1.9 µM).

The red solid line represents a theoretical protection profile calculated using the fitted MWC

model parameters for α1β2M286Cγ2L (Table 1). Open probability was calculated as a function

of [etomidate] at GABA = 2mM, protection was calculated using the predicted open-state

etomidate dissociation constant ($K_E \times d \approx 1.4$ µM) and a Hill slope of 1.0, and control

modification rate was set at the experimentally observed value (11,300 $M^{-1}s^{-1}$).

Tables

Table 1: Pharmacological, Kinetic and MWC Co-agonist Model Parameters for

$\alpha1\beta2\gamma2L$ and $\alpha1\beta2M286C\gamma2L$ GABA$_A$ Receptors

Parameter	$\alpha1\beta2\gamma2L$ Mean ± sd (n) [a]	$\alpha1\beta2M286C\gamma2L$ Mean ± sd (n)
GABA EC$_{50}$ (µM)	37 ± 17 (7)	210 ± 35 (6) **
nH	1.6 ± 0.39 (7)	1.5 ± 0.33 (6)
GABA Efficacy (%) [b]	88 ± 5 (4)	64 ± 4.2 (4) **
GABA EC$_{50}$ Shift with 3.2 µM Etomidate [c]	19 ± 7.8 (7)	2.7 ± 0.75 (4) **
Etomidate EC$_{50}$ (µM)	30 ± 11 (6)	na
Etomidate Efficacy (%)	45 ± 12 (6)	< 1 (4) **
Maximal Activation Rate (s^{-1})	3000 ± 1200 (4)	2500 ± 940 (4)
Fast desensitization Rate (s^{-1})	20 ± 13	16 ± 9.4
Amplitude (%)	30 ± 11 (4)	30 ± 18 (4)
Slow desensitization Rate (s^{-1})	1.0 ± 0.45	0.8 ± 0.29
Amplitude (%))	70 ± 11 (4)	70 ± 17 (4)
Fast deactivation Rate (s^{-1})	50 ± 18	57 ± 27
Amplitude (%)	60 ± 17 (4)	70 ± 17 (4)
Slow deactivation Rate (s^{-1})	6 ± 2.5	4 ± 2.7
Amplitude (%)	40 ± 17 (4)	30 ± 17 (4)
L$_0$ [d]	25,000	75,000
K$_G$ (µM)	70 ± 22	270 ± 46 **
c	(1.9 ± 0.38) x 10^{-3}	(2.4 ± 0.15) x 10^{-3}
K$_E$ (µM)	40 ± 14	12 ± 2.4 *
d	(7.6 ± 1.0) x 10^{-3}	0.12 ± 0.018 **

MOL #84558

[a] n is the number of separately analyzed experiments in individual oocytes, patches or cells used to calculate averages and errors. Average values for wild-type include previously published data from Stewart et al (2008), and Desai et al (2009).

[b] GABA Efficacy was determined as the ratio of maximal GABA current to current elicited with maximal GABA + 2 µM alphaxalone.

[c] EC_{50} shift is the ratio of GABA EC_{50} in the absence vs presence of 3.2 µM etomidate. Large values indicate significant positive modulation. A value of 1.0 represents no modulation.

[d] MWC model parameters were derived from fits of Eq. 3 to estimated P_{open} values (see methods and Figure 2).

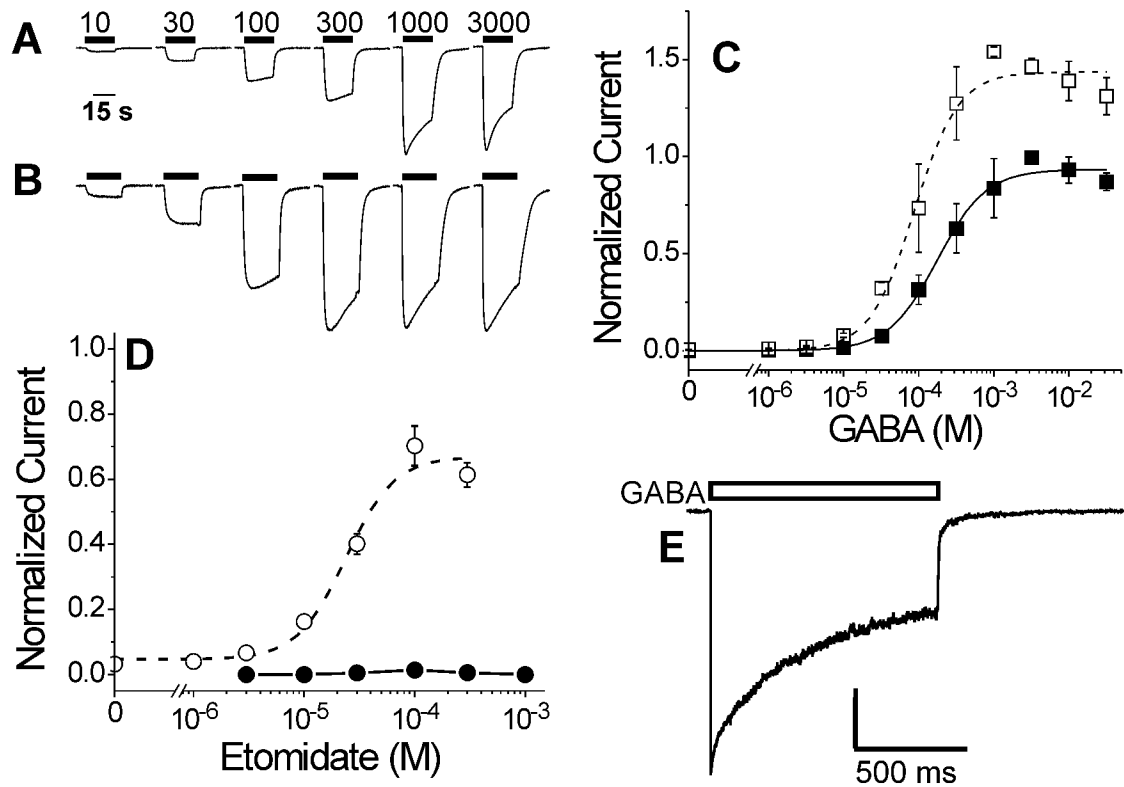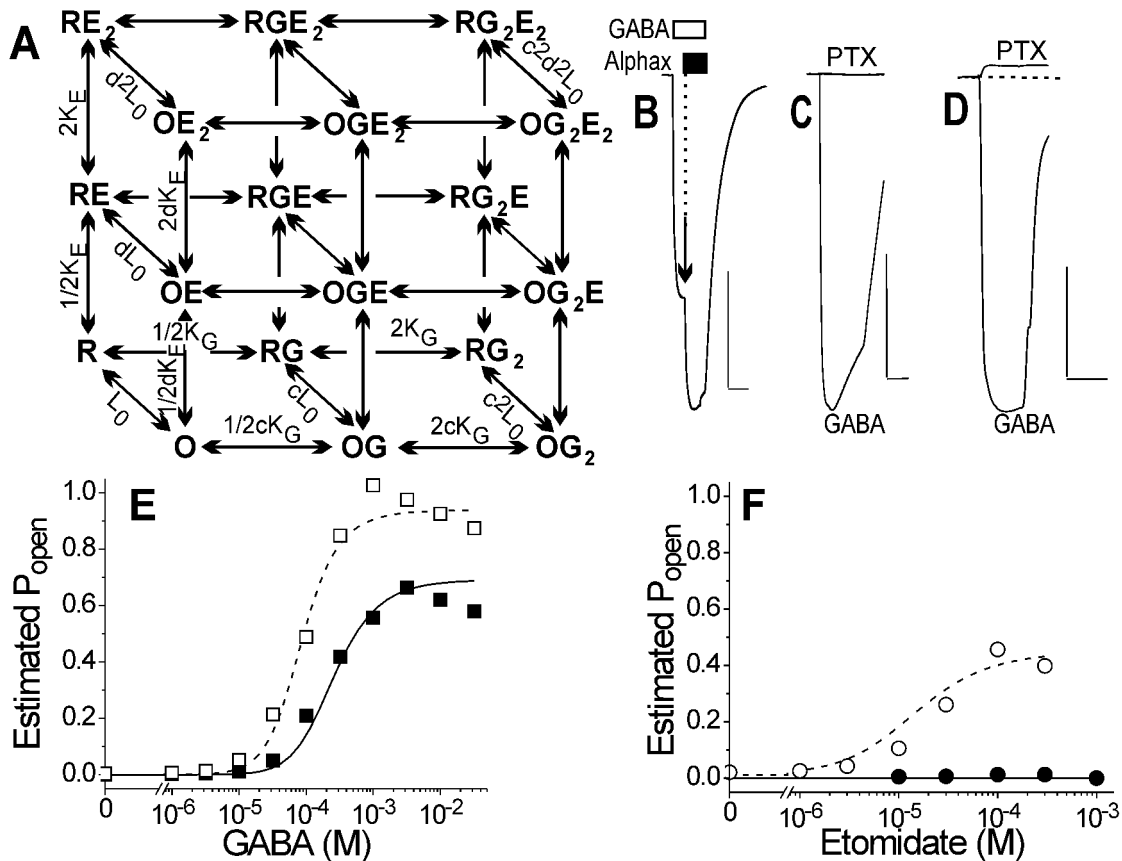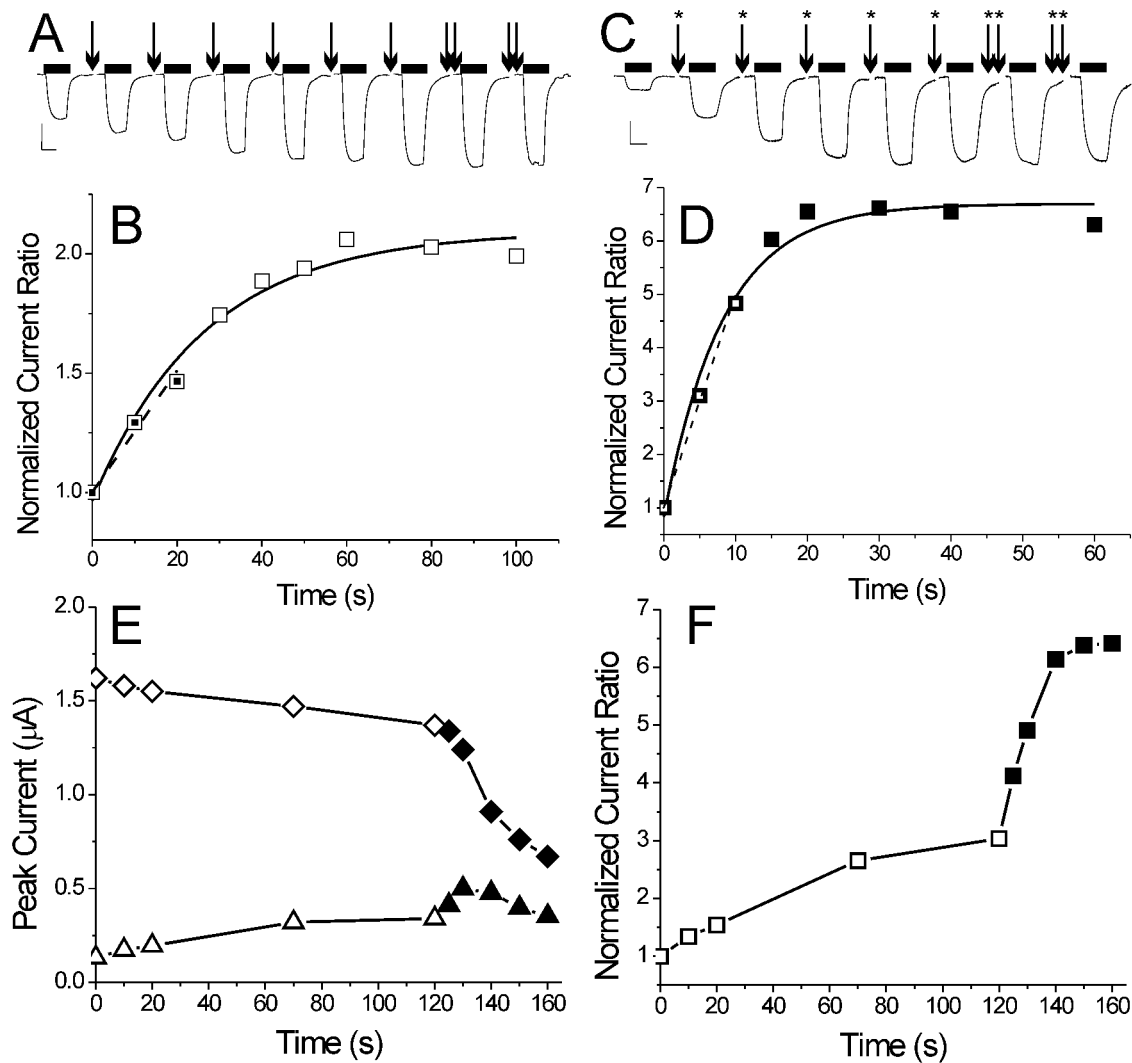* $p < 0.05$; ** $p < 0.01$

Figure 1

Figure 2

Figure 3

Figure 4